Icarus 264 (2016) 172–183

Contents lists available at ScienceDirect

Icarus

journal homepage: www.journals.elsevier.com/icarus

Bidirectional reflectance spectroscopy of carbonaceous chondrites: Implications for water quantification and primary composition

A. Garenne [a,b,*], P. Beck [a,b], G. Montes-Hernandez [c,d,e,f], O. Brissaud [a,b], B. Schmitt [a,b], E. Quirico [a,b], L. Bonal [a,b], C. Beck [g], K.T. Howard [h,i]

[a] Univ. Grenoble Alpes, IPAG, F-38000 Grenoble, France
[b] CNRS, IPAG, F-38000 Grenoble, France
[c] Univ. Grenoble Alpes, ISTerre, F-38000 Grenoble, France
[d] CNRS, ISTerre, F-38000 Grenoble, France
[e] IRD, ISTerre, F-38000 Grenoble, France
[f] IFSTTAR, ISTerre, F-38000 Grenoble, France
[g] CNRS ISTerre, Univ. Savoie-Mont-Blanc, 73376, Le Bourget du Lac, France
[h] Kingsborough Community College of the City University of New York, 2001 Oriental Blvd., Brooklyn, New York, NY 11235, USA
[i] Department of Earth and Planetary Sciences, American Museum of Natural History, New York, NY 10024, USA

ARTICLE INFO

Article history:
Received 21 April 2015
Revised 2 September 2015
Accepted 2 September 2015
Available online 12 September 2015

Keywords:
Meteorites
Asteroids
IR spectroscopy
Mineralogy

ABSTRACT

In this study, we measured bidirectional reflectance spectra (0.5–4.0 μm) of 24 CMs, five CRs, one CI, one CV, and one C2 carbonaceous chondrites. These meteorites are known to have experienced an important variability in their relative degrees of aqueous alteration degree (Rubin et al. [2007]. Geochim. Cosmochim. Acta 71, 2361–2382; Howard et al. [2009]. Geochim. Cosmochim. Acta 73, 4576–4589; Howard et al. [2011]. Geochim. Cosmochim. Acta 75, 2735–2751; Alexander et al. [2013]. Geochim. Cosmochim. Acta 123, 244–260). These measurements were performed on meteorite powders inside an environmental cell under a primary vacuum and heated at 60 °C in order to minimize adsorbed terrestrial water. This protocol allows controlling of atmospheric conditions (i.e. humidity) in order to avoid contamination by terrestrial water. We discuss various spectral metrics (e.g. reflectance, band depth, single-scattering albedo, ...) in the light of recent bulk composition characterization (Howard et al. [2009]. Geochim. Cosmochim. Acta 73, 4576–4589; Howard et al. [2015]. Geochim. Cosmochim. Acta 149, 206–222; Alexander et al. [2012]. Science 337, 721; Beck et al. [2014]. Icarus 229, 263–277; Garenne et al. [2014]. Geochim. Cosmochim. Acta 137, 93–112). This study reveals variability of reflectance among meteorite groups. The reflectance is not correlated with carbon or hydrogen abundance neither with measured grain size distribution. We suggest that it is rather controlled by the nature of accreted components, in particular the initial matrix/chondrule proportion. Band depth, integrated band depth, mean optical path length, normalized optical path length, effective single-particle absorption thickness were calculated on the so called 3-μm band for reflectance spectra and for single scattering albedo spectra. They were compared with hydrated phase proportions from previous study on the same meteorites by thermogravimetric analyses and infrared spectroscopy in transmission. We find that normalized optical path length (NOPL) is the most appropriate to quantify water abundance, with an absolute error of about 5 wt.%. These datasets also reveal a variability of the band shape between 2.8 and 2.9 μm, which is interpreted as reflecting variation in the chemical composition and structure of phyllosilicates. This chemical variation could also be used to quantify the aqueous alteration degree between meteorite groups. The combination of reflectance at 2 μm and the depth of 3-μm band can be combined, to classify carbonaceous chondrites in reflectance in term of primary composition (e.g. matrix/chondrule ratio, carbon content) and secondary processes (e.g. aqueous alteration, thermal metamorphism). This could be used to decipher the nature of aqueous alteration in C-complex asteroids.

1. Introduction

Asteroids contain refractory materials that are expected to have only been marginally affected by chemical processes since the

* Corresponding author at: Univ. Grenoble Alpes, IPAG, F-38000 Grenoble, France.
E-mail address: alexandre.garenne2@gmail.com (A. Garenne).

http://dx.doi.org/10.1016/j.icarus.2015.09.005
0019-1035/

formation of the Solar System. They can be considered as geological antiques that are expected to preserve precious clues to the birth of our planetary system. The main-belt is spectroscopically diverse suggesting that a variety of mineralogical compositions is present. Large spectroscopic surveys combined with dynamical studies have led to the classification of asteroid families (taxons), some of which have related meteorite groups (Tholen, 1984; Bus and Binzel, 2002; Gaffey et al., 1993; Vilas, 1994; Burbine, 1998; McSween et al., 2002; DeMeo and Carry, 2014). However, in the case of the darkest objects (the C-complex, and the D-types from DeMeo et al. (2009)) associations to specific meteorite groups can be difficult, because of the lack of diagnostic absorptions in the visible and near-infrared (VNIR).

Major spectroscopic surveys are limited to the VNIR and typically lack the 3-μm feature, which is the most diagnostic for –OH/H_2O bearing phases (water–ice, hydrated hydroxylated minerals, alcohol function). Such "water" related absorptions have been observed on asteroidal surfaces (Lebofsky et al., 1981; Larson et al., 1983; Jones et al., 1990; Rivkin et al., 2002), but observations in this region are usually limited to large objects and the effort of building a taxonomy based on this spectral range is ongoing (Takir and Emery, 2012). At present, most observations at 3-μm have been interpreted by the presence of –OH bearing mineral phase, and a few of them by the presence of water ice (mostly outer main belt objects, Campins et al., 2010; Rivkin and Emery, 2010; Takir and Emery, 2012; see also Beck et al. (2011) for an alternative – goethite). Across the main belt, 3-μm absorption bands have been found for different asteroid classes with variations in band shape and band depth (Takir and Emery, 2012; Rivkin et al., 2003). Some other asteroid classes do not present detectable 3-μm absorption features.

Some meteorite groups also show clear evidence of hydration in the form of secondary minerals formed under low-temperature, by precipitation from an aqueous fluid. This is particularly evident for some carbonaceous chondrite classes, including the CI group. The CI group is an extreme case of aqueously altered meteorites since almost all primary minerals were transformed to secondary phase, including phyllosilicates (a mixture of clays and serpentine; Tomeoka and Buseck, 1988). This aqueous alteration event was heterogeneous across the different carbonaceous chondrite families and within a given group. From the nature and amounts of secondary mineral phases, alteration sequences have been discussed (e.g. McSween, 1979; Bunch and Chang, 1980; Tomeoka and Buseck, 1985; Zolensky and McSween, 1988; Takir et al., 2013). Recently, aqueous alteration scales have been constructed based on petrography and crystal chemistry (Rubin et al., 2007; Harju and Rubin, 2013), phyllosilicate abundance (Howard et al., 2009, 2011, 2015; Beck et al., 2014; Garenne et al., 2014) and C and H isotopic analyses (Alexander et al., 2012, 2013).

Our objective here is to compare the spectral metrics of aqueously altered carbonaceous chondrites in reflectance, with an emphasis on the 3-μm region for comparison with remote observations of small bodies. The reflectance spectra were measured using a set of 23 CMs, 5 CRs from Antarctica and 4 chondrite falls (Orgueil (CI), Murchison (CM), Allende (CV) and Tagish Lake (C2)). Spectra were obtained under vacuum and moderate temperature to minimize contamination by adsorbed water, and with a high photometric accuracy (<0.25%). These same specific samples of each meteorite were previously studied by infrared spectroscopy in transmission (Beck et al., 2014) and with thermogravimetric analyses (Garenne et al., 2014) to evaluate modal mineralogy and water abundance. Many of these meteorites also had modal abundances determined by X-ray diffraction, although on different powder aliquots. Based on these two studies, we calculate various spectral metrics related to the 3-μm band and try to identify the most reliable way to quantify hydrogen on these dark meteorites and improve our understanding of the variability of the 3-μm band on low albedo asteroids.

2. Methodology, samples and analytical procedures

2.1. Meteorite samples studied

Reflectance spectroscopy was performed on 24 CMs, 5 CRs, 1 CI and 1 CV and one C2 chondrites (Table 1). Here we focused in particular on CM, CR and CI chondrites since they have been described in several articles as being significantly altered meteorites groups. These three groups have very distinct petrographical properties, different matrix proportion, carbon content, abundances of opaque phases, metal, secondary mineral phases, and water content (Brearley, 2006; Weisberg and Huber, 2007; Bunch and Chang, 1980; Zolensky and McSween, 1988; Krot et al., 2007). Their mineralogy and alteration degree have been studied previously (Bunch and Chang, 1980; Zolensky and McSween, 1988; Tomeoka et al., 1989; Browning et al., 1996; Rubin et al., 2007; Howard et al., 2009, 2011, 2015; Barber, 1981; Tomeoka and Buseck, 1985; Cloutis et al., 2011a,b, 2012, 2012b; Takir et al., 2013). The CM chondrites we analyzed were selected to span the full range of aqueous alteration from 2.0 to 2.6 defined by Rubin et al. (2007) and phyllosilicates range from 65 vol.% to 87.5 vol.% (Howard et al., 2011). One is a fall chondrite (Murchison) while some others was subjected to thermal events, like ALH 84033 and EET 83355. The CR chondrites studied cover a large range of aqueous alteration intensity from highly altered to primitive meteorites. Most of them are classified as CR2 except for GRO 95577, which is a CR1. EET 92159 has a primitive mineralogy (Abreu and Brearley, 2010) while RBT 04133 and GRA 06100 are spectrally different in the infrared (Beck et al., 2014). In the case of GRA 06100, the meteorite has been heated and shocked (Abreu and Stanek, 2009; Alexander et al., 2013).

Around 1 g of each meteorite was crushed and some part was used for the three methods; around 10 mg for thermogravimetric analyses (TGA), 1 mg for infrared spectroscopy in transmission and 700 mg for reflectance spectroscopy (Beck et al., 2014; Garenne et al., 2014).

2.2. H_2O/OH abundance determination

Three different methods were used to characterize the nature of aqueous alteration in our suite of chondrites: thermogravimetric analyses (TGA) (Garenne et al., 2014), infrared (IR) spectroscopy in transmission (Beck et al., 2014) and reflectance spectroscopy. TGA measurements were used to quantify water abundance, to identify the mineral host of water and the level of matrix aqueous alteration (Garenne et al., 2014). Infrared spectroscopy was used to identify the mineralogy from the silicate vibration modes and to quantify (–OH) abundance based on the 3-μm band (Beck et al., 2014). This paper presents the reflectance spectra of the same sample aliquots studied by TGA and transmission IR methods. This approach was used to minimize the chemical and mineralogical variations due to the heterogeneity of the meteorites (most of them are regolith breccia; Bischoff et al., 2006), and to avoid possible nugget effects. This heterogeneity was measured and quantified on one CM chondrite by thermogravimetric analyses and it is estimated at 0.95 wt% on H_2O quantification (for a sample containing an average of 5.3 wt% of H_2O in phyllosilicates, 6 measurements) (Garenne et al., 2014). The IR spectroscopy and TGA results allow us to constrain our reflectance spectra and to find the best spectral metrics to quantify the water abundance with the reflectance spectroscopy. In addition, the hydrogen content (H_2O/OH contributions) estimated by Alexander et al. (2012, 2013) from bulk H and C measurements were used to trace the impact of parent body process on reflectance spectra features.

Table 1
Summary of chondrites studied with their type, weathering grade, petrological grade, grain size and reflectance at 1 μm. Samples designed as heated CM chondrites were recognized as so by Alexander et al. (2013).

	Type/subtype	Fall/*find*	Weathering grade	Petrologic grade	Volume weighted mean (μm)	Reflectance at 1 μm
CI						
Orgueil	CI	Fall	–	1		0.0581516
CR						
GRO 03116	CR	*find*	B/C	2	105.417	0.123499
GRA 06100	CR	*find*	B	2	132.473	0.100974
GRO 95777	CR	*find*	B or B/C	1	102.878	0.117483
RBT 04133	CR	*find*	B/C	2	142.245	0.0852997
EET 92159	CR	*find*	B/C	2	119.305	0.0913078
CV						
Allende	CV	Fall	–	3	424.244	0.0932192
CM						
ALH 83100	CM	*find*	Be	1/2		0.0662016
ALH 84029	CM	*find*	Ae	2		0.0604111
ALH84044	CM	*find*	Ae	2		0.0767213
DOM 08003	CM	*find*	B	2	146.555	0.0683007
LAP 02333	C2/CM	*find*	A/Be	2	120.972	0.0770358
LAP 02336	CM	*find*	B	2	131.322	0.0744609
LAP 03718	CM	*find*	BE	2	176.583	0.0687636
LEW 85311	C2/CM	*find*	Be	2	55.398	0.0545367
LEW 85312	C2/CM	*find*	B	2	67.262	0.0500835
LEW 87022	CM	*find*	B	2	93.882	0.0542591
LEW 90500	C2/CM	*find*	B	2	84.931	0.0554436
LON 94101	C2/CM	*find*	Be	2		0.0567994
MET 01070	CM	*find*	Be	1/2.0	195.123	0.0506628
QUE 97990	CM	*find*	Be	2/2.6		0.0479868
Murchison	CM	*Fall*	–	2/2.5	196.857	0.0633829
Heated CM						
ALH 84033	CM	*find*	Ae	2	133.401	0.0744234
DOM 03183	CM	*find*	B	2	137.994	0.0700602
EET83355	C2	*find*	A/B	2	122.609	0.069471
EET 96029	C2/CM	*find*	A/B	2		0.0591659
EET 87522	CM	*find*	Be	2	85.283	0.0486964
MAC 88100	CM	*find*	Be	2	56.952	0.0465085
MIL 07700	CM	*find*	A	2	136.896	0.0445215
PCA 02012	CM	*find*	B	2		0.096659
WIS 91600	C2/CM	*find*	A/Be	2	143.762	0.0408526
Ungrouped C2						
Tagish Lake	C2	*Fall*	–	2	229.408	0.041

2.3. Grain size

Because we were interested in analogs of asteroidal surfaces, there were no grain sorting or sieving performed. In this light our meteorite powders are heterogeneous and contain a continuum of grain size as expected on asteroid surfaces. To determine possible grain size effects, grain size distribution was characterized by laser granulometry for each sample. The grain-size spectrum of each powder was measured with a MALVERN™ Mastersizer 2000 laser-granulometer (combining red and blue lights diffraction) with a 0.02–2000 μm range. Measurements were realized as suspension with water as dispersant, and without ultrasonic treatment. The grain size was automatically calculated by the software Malvern Mastersizer 2000. The volume weighted mean is presented in Table 1.

2.4. Reflectance spectroscopy

For each meteorite around 1 g was manually crushed in an agate mortar. The same preparation protocol was followed for each meteorite sample. About 700–900 mg of meteorite powder was necessary to fill the sample holder. This mass is large enough so that the optical depth can be considered as infinite (Pommerol and schmitt, 2008a,b). A smooth sample surface was prepared carefully to limit texture effects on the reflectance spectra (e.g. Cord et al., 2003, 2005; Shkuratov and Grynko, 2005). The samples were inserted in an environmental chamber under primary vacuum and heated at 60 °C in order to minimize contamination by adsorbed terrestrial water. All measurements were performed under these conditions, spectra were acquired after the pressure and temperature were stable (typically 30 min).

All reflectance spectra were measured with the Laboratoire de Planétologie de Grenoble (LPG) Spectro-gonio-radiometer (Brissaud et al., 2004). This instrument can measure reflectance spectra in the visible and near infrared with a spectral range from 0.5 to 4.0 μm. Spectra were measured with a spectral sampling step of 20 nm and typical resolution of 5–40 nm depending on the wavelength. All spectra were recorded with an incidence angle of 0°, an emergence angle of 30° and an azimuth angle of 0° (principal plane). The calibrations of the reflectance spectra were performed by dividing each spectrum by the spectra of reference surfaces (Spectralon and Infragold from Labsphere Inc.).

The typical acquisition time of an individual spectrum is one hour. For each meteorite, between 10 and 20 spectra were recorded and averaged to reduce the signal to noise ratio.

2.5. Spectral metrics

2.5.1. Band depth

The most common criterion used in reflectance spectroscopy to determine the strength of absorption is the relative band depth (Clark and Roush, 1984)

$$BD(\lambda) = 1 - \frac{R(\lambda)}{R_c(\lambda)}$$

where $R(\lambda)$ is the reflectance at the specific wavelength, in this case between 2.8 and 3.1 μm (generally chosen in the maximum of absorption), $R_c(\lambda)$ the value of reflectance for a continuum at the same wavelength. The continuum is defined as a constant value taken as the reflectance at 2.64 μm for each meteorite corresponding to the maximum reflectance region.

2.5.2. Integrated band depth

The Integrated Band Depth (IBD) takes into account the full "energy" of the band by integrated band depth over a specific spectral range. In our case we have chosen a range between 2.8 and 3.1 μm including OH from phyllosilicates and H_2O, which can be calculated for Earth based observations without pollution from atmospheric water. As recommended by Milliken and Mustard (2005), the IBD is normalized to the total possible area of absorption, allowing for more direct comparisons with other absorption bands.

$$IBD_\lambda = \frac{\int_{\lambda_{min}}^{\lambda_{max}} 1 - \frac{R(\lambda)}{R_c(\lambda)} \cdot d\lambda}{\int_{\lambda_{min}}^{\lambda_{max}} BD_{max.poss.}(\lambda) \cdot d\lambda} = \frac{\int_{\lambda_{min}}^{\lambda_{max}} BD(\lambda) \cdot d\lambda}{\lambda_{max} - \lambda_{min}}$$

2.5.3. Mean optical path length

In transmission, the amount of light penetrating the sample is defined by $= e^{-\propto x}$, where α is the absorption coefficient and x is the optical path length $x = -\frac{1}{\propto}\ln(t)$. From this Kortum (1969) defined an analogue criterion called effective absorbance $A_e = -\ln(R)$, where R is the reflectance. Clark and Roush (1984) define the mean optical path length as $MOPL = \frac{A(e)}{\propto} = -\frac{1}{\propto}\ln(R)$. The absorption coefficient for a specific wavelength is defined by $\propto(\lambda) = \frac{4\pi k(\lambda)}{\lambda}$, where k is the imaginary part of the refraction index. We used for the 3 μm region a value of $k = 0.28234$ at $\lambda = 2.951$ μm (Milliken and Mustard, 2005). We also used for the reflectance value, a normalization defined by the continuum, obtained as follows:

$$MOPL_\lambda = -\ln\left(\frac{R(\lambda)}{R_c(\lambda)}\right) \cdot \frac{\lambda}{4\pi k(\lambda)}$$

2.5.4. Normalized optical path length

This parameter introduced by Milliken and Mustard (2005) is based on the MOPL where the exponential term of Beer's law is taken relative to a continuum reflectance instead of 1. They define it like this:

$$NOPL_\lambda = \frac{-\ln[R(\lambda) + 1 - R_c(\lambda)]}{-\ln[1 - R_c(\lambda)]}$$

In their studies, Milliken and Mustard (2005, 2007) used the mass loss upon heating of their samples to quantify the water abundance and to compare with the different metrics calculated from reflectance spectra. From theory the NOPL is expected to be correlated linearly with absorption coefficient (Hapke, 2012), and it was shown to be a good proxy for water abundance in these articles.

2.5.5. Particle single scattering albedo

The particle single scattering albedo, w, represents the interaction of the light with a single particle, considering a proportion of this light is adsorbed by the particle and the other proportion is scattered. w is then defined by the proportion of scattered light relative to the incident light (Hapke, 2012):

$$w = Qs/Qe$$

With Qs being the scattering efficiency and Qe the extinction efficiency. Hapke (2012) shows that the bidirectional reflectance is related to the single scattering albedo by:

$$r(i,e,g) = K\frac{w}{4\pi}\frac{\mu_0}{\mu+\mu_0}\{p(g)[1 + B_{s0}B_s(g)] + [H(\mu_0/K)H(\mu/K) - 1]\} \times [1 + B_{c0}B_s(g)]$$

Given our observation geometry (emergence angle, $e = 30°$ and incidence angle $i = 0°$), it is reasonable to assume the absence of opposition effects ($B(g) = 0$). If the hypothesis that the particles scatter isotropically ($P(g) = 1$) is also used, then:

$$r(i,e,g) = K\frac{w}{4\pi}\frac{\mu_0}{\mu+\mu_0}[H(\mu_0/K)H(\mu/K) - 1]$$

where $H(x)$ is the Ambartsumian-Chandrasekhar function which can be approximate by $\frac{1+2x}{1+2x\gamma}$ with γ is the albedo factor defined by $w(\lambda) = 1 - \gamma(\lambda)^2$.

In our study we measured reflectance relative to the spectralon, a nonabsorbing, highly lambertian, medium. If it is assumed that there is negligible difference in the porosity coefficient, K, between the sample and the standard, the relative bidirectional reflectance is given by:

$$R(i,e,g) = \frac{w}{(1 + 2\gamma\mu_0)(1 + 2\gamma\mu)}$$

Solving for $\gamma(\lambda)$ it is:

$$\gamma(\lambda) = \frac{\sqrt{(\mu+\mu_0)^2R(\lambda)^2 + (1 + 4\mu\mu_0R(\lambda))(1 - R(\lambda))} - (\mu+\mu_0)R(\lambda)}{1 + 4\mu\mu_0R(\lambda)}$$

With $w(\lambda) = 1 - \gamma(\lambda)^2$, $\mu = \cos(e), \mu_0 = \cos(i)$.

All reflectance spectra were converted into Single Scattering Albedo (SSA) and the spectral metrics described before for the 3-μm absorption band were calculated for the SSA spectra. This method has the inconvenience of making a number of hypothesis/assumptions (e.g. isotropical scatter, equal porosity between sample and standards) but the advantage is that it minimizes albedo dependence and increases exponentially the band depth. This approach has been shown to be an efficient way to quantify water abundance (Milliken and Mustard, 2007), and this conversion allows introducing a valuable parameter, the effective single particle absorption thickness.

2.5.6. Effective single-particle absorption thickness

This function is only defined for single scattering albedo. When k, the extinction coefficient is equal to 1, the light absorbed must be proportional to the product of the absorption coefficient and the volume of the particle (Hapke, 2012). This is indeed true in the range $\alpha D < 0.1$ with D, the average distance traveled by the particle (Hapke, 2012). From the definition of the single scattering albedo, Hapke deduces:

$$ESPAT(\lambda) = W(\lambda) = \frac{1 - w(\lambda)}{w(\lambda)}$$

If αD is linearly proportional to water content, this function should be proportional too.

3. Results

3.1. Reflectance spectra of Antarctic CMs

All spectra acquired for CM chondrites (excluding the fall Murchison) are presented in Fig. 1. CM reflectance spectra are characterized by five typical criteria (Cloutis et al., 2011b): (1) A

generally low reflectance (R); (2) A deep 3-μm band due to hydration (hydroxylated minerals, H_2O-bearing minerals); (3) a silicate band at 0.7 μm due to Fe^{3+}–Fe^{2+} charge transfer; (4) a silicate band around 0.9–1.2 μm due to Fe^{2+} crystal field transitions; (5) a band around 3.4–3.5 μm which can be assigned to organic matter. These five criteria are not always all observed for a given sample.

The spectra obtained show variations in the reflectance typically varying between, 0.04 and 0.08 for non-heated CMs (at 1 μm). All spectra show a pronounced 3-μm feature extending typically between 2.7 and 3.8 μm and the minimum reflectance is achieved between 2.7 and 2.9 μm and varies between 0.024 and 0.05 (again, for non-heated CM chondrites). In our dataset a broad absorption between 0.5 and 1.5 μm might be present. Given our spectral resolution it is not clear if it is attributed to the combination of the 0.7 μm feature caused by Fe^{3+}–Fe^{2+} charge transfer, together with the crystal field band due to octahedral Fe^{2+} ion (between 0.9 and 1.2 μm), as was previously observed for CM chondrites (Cloutis et al., 2011b).

In some CM spectra, an absorption feature is seen between 3.4 and 3.5 μm (Fig. 1), which seems to be related to the presence of a smaller feature around 2.5 μm. The feature at 3.4–3.5 can be explained by the presence of organics absorptions (e.g., aliphatic CH stretching that has been documented for CM chondrites; Orthous-Daunay et al., 2013). However this feature can be mixed with vibration overtones from carbonate group minerals, and, given our spectral resolution, the distinction between carbonates and organics is difficult.

Finally, it should be noted that the metal-OH feature at around 2.2–2.3 μm, which is often used to identify phyllosilicates in remote sensing (particularly on Mars, Bibring et al., 2006; Carter et al., 2010), is not present in any CM chondrite spectra, despite the fact that their mineralogy is dominated by phyllosilicates. The reason for the lack of such a feature could be the presence of opaque phases that "hides" weak absorptions. Another possibility is that this feature is absent because of the very low crystallinity of the phyllosilicates, which was observed from the shape of the 10-μm silicate feature (Beck et al., 2010) and is reported in XRD studies (Howard et al., 2009).

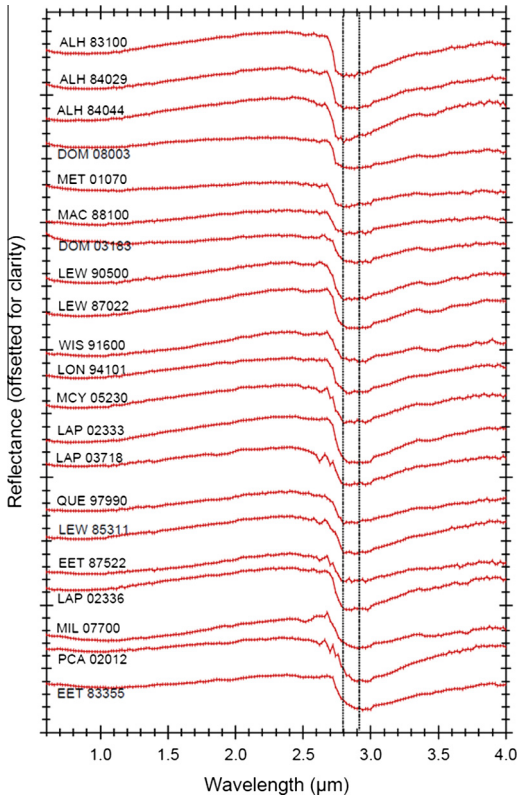

Fig. 1. Reflectance spectra of the CM chondrites studied. Spectra were offsetted for clarity.

3.2. Reflectance spectra of CRs

The reflectance spectra of CRs are presented in Fig. 2. In comparison to CM chondrites, the reflectance is generally higher (between 0.085 and 0.125 at 1 μm, Fig. 2). Of the five CRs studied, the CR1 shows the lowest reflectance at 1 μm.

The reflectance spectra obtained for EET 92159 and GRO 03116 shows a small absorption feature at around 0.9–1.0 μm that has been previously observed for CR chondrites (Cloutis et al., 2011a). The maximum of absorption of this feature is at a wavelength shorter than that of olivine, and has been interpreted to reflect the presence of Fe-oxide, Fe-hydroxide or Fe-oxy-hydroxide (Cloutis et al., 2011a), probably of terrestrial origin. The presence of a such mineral phase in EET 92159 and GRO 03116 is reinforced by the presence of a red visible slope for these two CR chondrites (Fig. 2). However, the presence of an olivine–pyroxene mixture could also explain the presence of an absorption feature at around 0.9–1 μm. As discussed in details in Cloutis et al., (2011a), one of the difficulties in interpreting CR chondrites is the impact of terrestrial weathering on this metal-rich meteorite group.

All CR samples studied show a deep 3-μm band, with the wavelength of maximum absorption in the CR1 GRO 95577 (at 2.8 μm) being distinct from the other studied CR (around 2.9–3.0 μm). The 3-μm band shape of the CR1 is similar of CM chondrites and can be interpreted to be mostly due to phyllosilicates. In the case of the CR chondrites, the position of the maximum of absorption at higher wavelength is consistent with the presence of Fe-hydroxide, or an Fe-oxy-hydroxide (Lair et al., 2006).

For the studied CR chondrites the 3.4–3.5 μm band features are weak and the band depth seems to be smaller than for CM chondrites (Fig. 2).

3.3. Reflectance spectra of fall chondrites

The spectra of four falls meteorites analyzed (Orgueil (CI), Allende (CV), Murchison (CM) and Tagish Lake (C2 ungrouped))

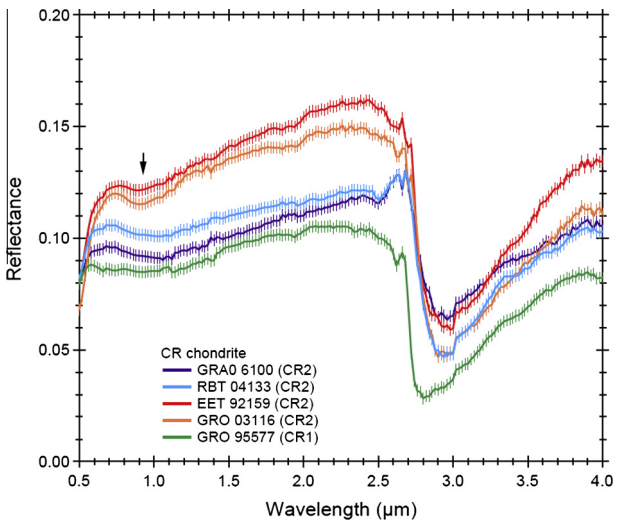

Fig. 2. Reflectance spectra of the CR chondrites studied. Spectra were offsetted for clarity. The arrow indicates putative Fe^{3+} related absorption. Note also the steeper visible slope in the case of GRO 03316 and EET 92159.

are presented in Fig. 3. These four samples belong to four different groups and have clearly distinct spectral characteristic in our wavelength range.

Among the four falls, Allende is the brightest, with a reflectance of 0.094 at 1 μm, and Tagish Lake is the darkest with a reflectance of 0.04 at 1 μm. The characteristics that dominate Allende spectra are a broad feature around 1 μm probably due to mafic olivine and a broad absorption feature between 1.6 and 2.4 μm explained by spinel bearing calcium–aluminum rich inclusion (Cloutis et al., 2012). All of our results are consistent with reflectance spectra obtained on CV chondrites previously (Cloutis et al., 2012). In addition, the spectra of Allende reveals a 3-μm absorption, much weaker than those of the CI, the CMs and Tagish Lake, which is consistent with a low abundance of phyllosilicates in Allende (3–4 vol. %) (Howard et al., 2010).

The spectra of Orgueil, Tagish Lake and Murchison all show a broad absorption feature, centered at 0.95 μm. The intensity of this feature decreases in the order Murchison > Tagish Lake > Orgueil. Such an absorption feature is present in the reflectance spectra of phyllosilicates with iron in a mixed valence state, where it is usually the combination of absorption at 0.7 and 0.9 μm. In the case of Murchison and Tagish Lake, it is probably mixed with absorption at 1 μm due to Fe-bearing olivines.

In the 3-μm region, the band shape appears different, although the SNR is high for these spectra. One clear difference between the spectra of Orgueil, Tagish Lake and Murchison is that the 3-μm band depth of Tagish Lake is clearly lower. These results seem to suggest that this matrix-rich meteorite could have experienced a thermal dehydration event as suggested by other workers (Alexander et al., 2014).

4. Discussion

4.1. What is controlling the reflectance of carbonaceous chondrites?

4.1.1. Grain size?

Grain size can have a first order effect on the reflectance spectra of pure minerals. In general, decreasing grains size tends to increase the number of scatterings and leads to an increase in reflectance. When the grain size approaches that of the incident wavelength, a change of scattering regime occurs leading to a decrease in reflectance (Mustard and Hays, 1997). In the case of carbonaceous chondrites, which are fine-scale mixture of components with contrasted optical properties, the grain size relevant to the reflectance spectra can be difficult to define. In a classical approach, the effect of grain size on the spectra is studied by means of analyzing a sieved, ground fraction of the meteorite. However, the various sieved fractions might not be isochemical or uniform in mineralogy. In this study grain size was not controlled through sieving, opting instead for a distribution of grain size which was estimated with a laser granulometer. The grain size distribution determined by this optical method is likely appropriate for the understanding of reflectance spectra.

From the grain size distribution, one can calculate the averaged grain size mode, using a surface weighted or a volume weighted average. These grain size was typically around 20–50 μm for the surface weighted and 100–200 μm for the volume weighted. If grains were devoid of internal scatters, the surface weighted mode might be the most relevant to characterize the effect of grain size on the reflectance spectra. However, because grains are more than likely to have internal scatterers, volume weighted mode was also estimated.

These two parameters are plotted against the reflectance at 1-μm, for the series of meteorites studied here (Fig. 4). Although there is some variability in grain size measured for the samples studied (typically between 50-μm and 200 μm volume average), no clear control of grain size on the reflectance is observed.

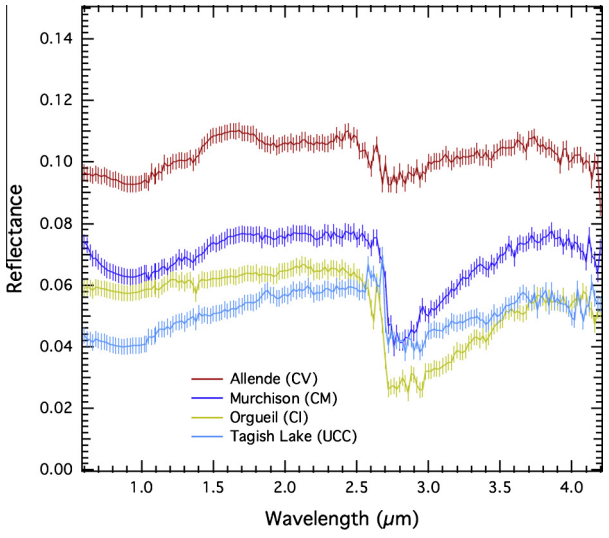

Fig. 3. Reflectance spectra of the falls studied. Spectra were offsetted for clarity.

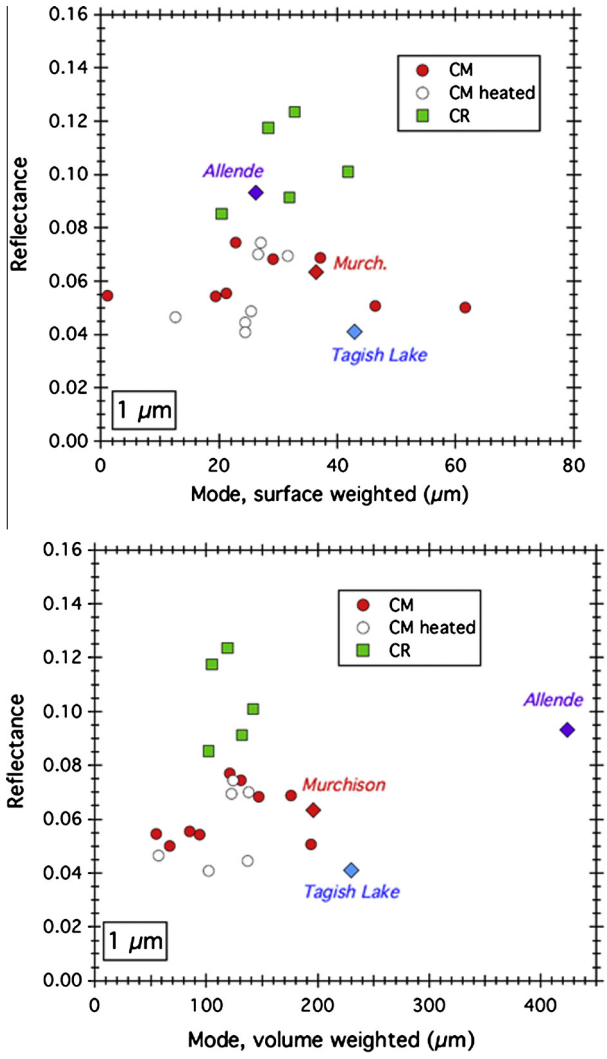

Fig. 4. Reflectance at 1-μm as a function of the grain size determined by laser granulometry.

4.1.2. Carbon content and maturity?

The abundance of carbon is variable among CC and can reach up to 6 wt% (Scott and Krot, 2007). Two organic carbon reservoirs are usually distinguished in the literature. The insoluble organic matter (IOM) is the fraction of organic matter that resists hard acid attack and is constituted by large macromolecular carbon compounds (Remusat et al., 2006). The soluble organic matter (SOM) is the counterpart of the IOM, and can be extracted with classical solvents. The relative proportions of C contributed by each reservoir are usually estimated as around 75–99% from IOM and 1–25% from SOM (Gilmour, 2003). When measuring the reflectance spectra of carbonaceous chondrites, both the SOM and the IOM are expected to contribute. Carbon seems a natural candidate as being one of the opaque phases responsible for the low albedo of carbonaceous chondrites. However, if most macromolecular carbons are dark in the visible, this is not always the case in the NIR spectroscopy as shown by studies of coals and bitumen (Cloutis et al., 2012; Moroz et al., 1998). Indeed, the later studies have shown that with increasing maturity, the visible optical gaps of coals and bitumen extends to the NIR region and that these terrestrials analogs become opaque through the full VNIR range.

In Fig. 5, the reflectance spectra at 2 μm are plotted against the bulk carbon content derived by Alexander et al. (2007). Across the studied CC groups, these results show a global trend where reflectance decreases as carbon content increases. This suggests that if macromolecular carbon is the dominant opaque for this series of CC, it has to be opaque from the visible to the NIR, and is therefore a relatively mature form of carbon by analogy with terrestrial coals and bitumen. Still, this appears unlikely given the state of knowledge of IOM thermal history (Quirico et al., 2014).

In addition, some metamorphosed CM chondrites did lose a major fraction of their IOM without a significant impact (Fig. 5). This tends to suggest that carbon is not the major darkening agent across the whole spectral range.

4.1.3. Aqueous alteration?

Because aqueous alteration induces the crystallization of secondary phases, some of which are opaques (tochilinites, sulfides, other oxides, ...), a possible relation between the reflectance and the level of aqueous alteration needs to be investigated. As a proxy to the level of aqueous alteration the water content was used (Howard et al., 2009; Alexander et al., 2013; Garenne et al., 2014; Beck et al., 2010). Fig. 6 shows the relation between the reflectance at 1 μm and the amount of water derived from bulk measurements by mass spectrometer, as well as with the –OH related absorption measured with infrared spectroscopy. In the case of the CM chondrites, although the amount of H_2O/–OH related hydrogen varies by a factor of two, there is no correlated variation of the reflectance. In the case of the CR chondrites, even though the CR1 has the least reflectance, the small number of samples precludes any firm conclusion.

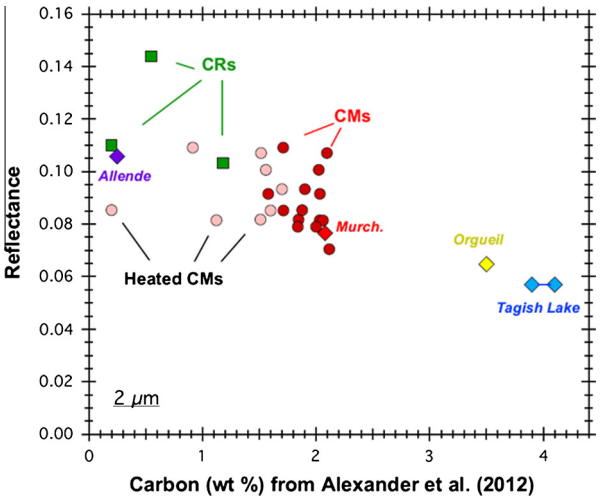

Fig. 5. Reflectance at 2-μm as a function of meteorite bulk carbon content, derived by Alexander et al. (2012, 2013).

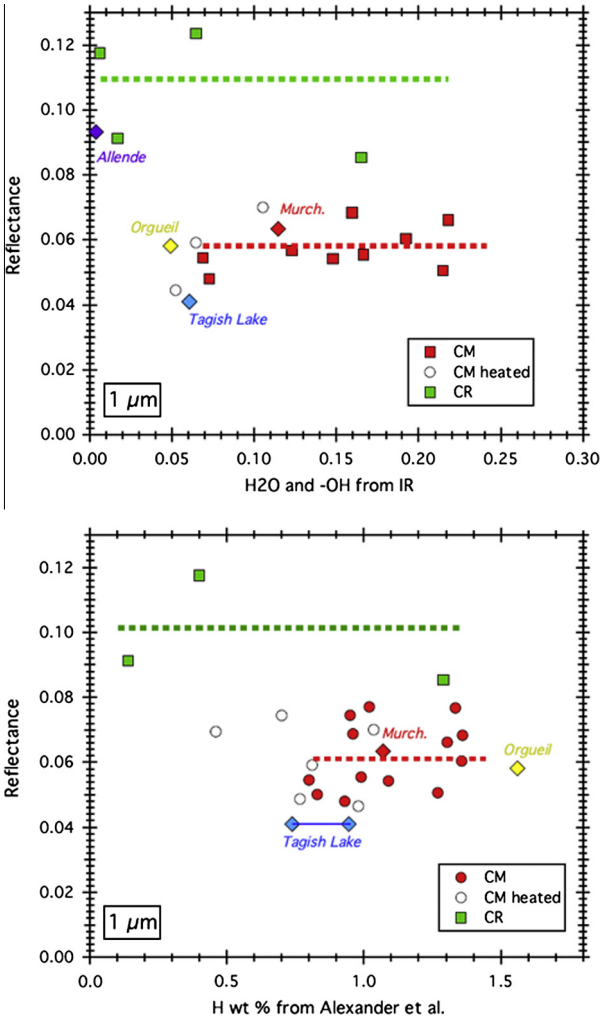

Fig. 6. Reflectance at 1-μm as a function of hydrogen or water content. Horizontal dashed lines are guides for the eye.

4.1.4. Primary mineralogy

The correlation between carbon contents and reflectance might be used to argue that IOM acts as a major darkening agent, but one should keep in mind that this correlation could simply indicate that the matrix is rich in opaque phases. Because chondrule have well crystalline silicate, large in size relative to the fine-grained matrix, it is reasonable to suggest that the reflectance across our series of chondrites is controlled by the relative amount of a bright component (chondrules) and a dark component (the matrix). Since, for the reasons described above (Section 4.1.2), carbon cannot be the only opaque (especially above 1 μm) other phases have to be invoked. The matrix is rich in opaque phases, including sulfides or iron oxides, and the bulk of the matrix is Fe-rich, and therefore even the silicates probably have high absorption coefficients; numerous phases can contribute to the darkness of the matrix.

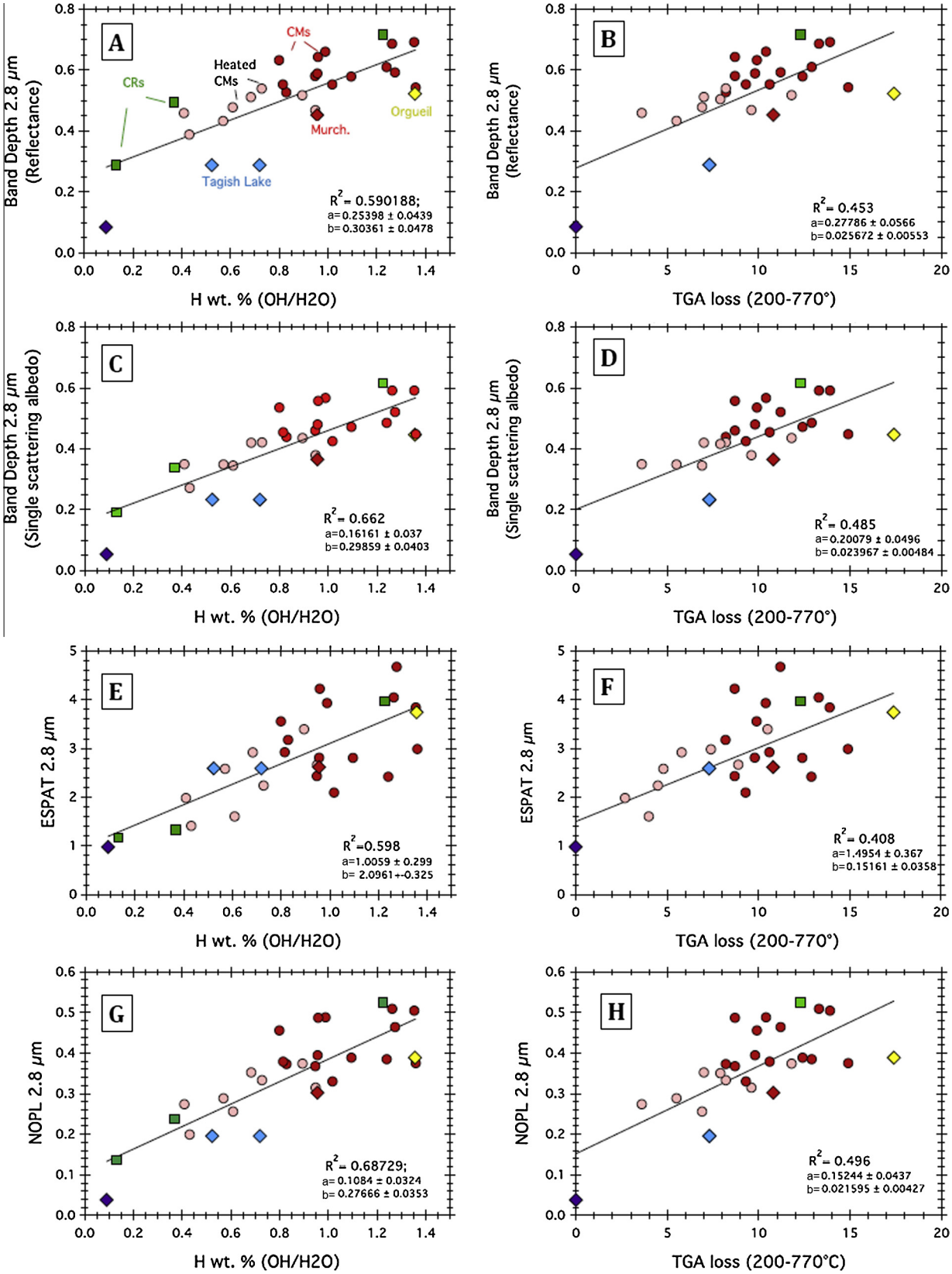

Fig. 7. Spectral criteria (see text) against the water (Garenne et al., 2014) or hydrogen content (Alexander et al., 2012).

4.2. Quantifying hydration with reflectance spectroscopy

Several criteria were tested following the detailed work of Milliken and Mustard (2005, 2007), as well as Pommerol and Schmitt (2008a,b). The criteria that will be discussed in the following paragraphs were chosen based on: (i) applicability to ground based observations of asteroid spectra, (ii) requirement of minimal spectral processing assumptions, and (iii) the quality

of the correlation found with water content based on a least square approach.

4.2.1. Band depth

Band depth is probably the simplest spectral criterion to investigate variability of spectral absorption. It is defined relative to a continuum reflectance, and can be calculated whether on the measured reflectance spectra or, once calculated, on Single Scattering Albedo (SSA) spectra. In principle, relative band depth has the advantage in being able to remove variations related to grain size but has the disadvantage of being strongly impacted by observation geometry at elevated incidence angle (Pommerol and Schmitt, 2008a; Beck et al., 2012), where absolute band depth is preferred.

Fig. 7A shows the relation between Band Depth at 2.8 μm (BD2.8) and H_2O/OH content as determined by Alexander et al. (2012, 2013) or from TGA loss (Garenne et al., 2014). As seen in all plots of Fig. 7, the relation between spectral criteria and water content is always better when using water quantification by Alexander et al. This is likely related to the higher uncertainty of TGA measurements, and the possible contribution of the decrepitation of sulfides. As seen in Fig. 7A, there is a fair correlation between BD2.8_REF and H_2O/OH hydrogen abundance. When taken as a whole, the meteorite suite suggest a relation rather logarithmic than linear. However, examination of this graph in more detail reveals that the relation between the BD2.8_REF criteria and H (H_2O/OH) content is albedo-dependent. The CR chondrites that have a higher continuum reflectance plot in the higher part of the diagram, while Tagish Lake and Orgueil, which have a lower continuum reflectance plot in the lower portion of the graph. Indeed, it has been shown in previous study that the 3-μm band depth can be strongly correlated to continuum reflectance from both laboratory measurements and planetary observations (Pommerol and schmitt, 2008a,b; Milliken and Mustard, 2007; Jouglet et al., 2007).

The band depth at 2.8 μm was then calculated in single-scattering albedo (BD2.8_SSA) (Fig. 7C and D). The relation between this criteria and H_2O/OH hydrogen seems to be slightly better than, with BD2.8_REF, however the dependence on continuum reflectance remains. For similar hydrogen content, the band depth of the CR is higher than that of CM, which themselves are higher than that of Orgueil.

4.2.2. Effective single-particle absorption thickness

According to Hapke (2012), the ESPAT criterion is expected to be linearly correlated with the absorption coefficient, and therefore should be the most appropriate for quantification. As shown in Fig. 7E, there is a rough correlation of ESPAT with H_2O/–OH hydrogen (R^2 = 0.602 for a linear correlation). The advantage of using ESPAT is that all types of carbonaceous chondrites studied spread on a single correlation space, and ESPAT seems to be independent of continuum reflectance. It could be virtually the most appropriate for remote quantification of water, but given the spread observed in Fig. 7, the accuracy of the method is limited. For a given value of ESPAT, the H_2O/OH hydrogen abundance can vary by more than a factor of 2.

4.2.3. NOPL

The NOPL (see Section 2.5.5) was calculated on reflectance spectra and on SSA spectra following Milliken and Mustard (2005). In the case of reflectance spectra, given the low reflectance values, the NOPL at 2.8 μm is identical to BD2.8 within a few percent and is therefore not shown. The NOPL at 2.8 μm in SSA scattering albedo is shown in Fig. 7G. The quality of the correlation obtained taking into account all samples is slightly better than with ESPAT (R^2 = 0.641 for a linear correlation) and there seems to be some overlap between data from different meteorite groups, unlike what is observed in the case of BD2.8. Nevertheless, given the spread of the data, for a given value of NOPL2.8 (SSA) water content can vary by 30–50%, which gives an idea of the accuracy we can expect by using this criterion for quantifying water content. Furthermore we have compared these results with the petrologic type recently proposed by Howard et al. (2015). This petrologic type was calculated by the normalized fraction of phyllosilicate measured by X-ray diffraction (Howard et al., 2015). Fig. 8 presents a comparison between the NOPL calculated at 2.8 μm and the petrologic type proposed by Howard et al. (2015). A reasonable correlation is found between the two methods though Murchison appears slightly of the correlation. Except this meteorite, the quality of the correlation for the other meteorite is good (R^2 = 0.69 without Murchison). The phyllosilicates of Murchison are different with a stronger cronstedtite/Fe–Mg phyllosilicates ratio than the find carbonaceous chondrites studied (Howard et al., 2015). This is also observed with the band geometry of Murchison, which reflects a different chemistry from its high BD 2.8 μm/2.9 μm ratio (Section 4.2.4). Therefore, it is suspected that the NOPL parameters at 2.8 μm depends of the phyllosilicate chemistry for a given waters content. Further studies on additional fall meteorites will be very useful for a better understanding of this difference.

4.2.4. Band geometry

In a previous work performed on a suite of CI and CM chondrite in transmission, it was found that the geometry of the 3-μm is not constant between carbonaceous chondrites and seems correlated with aqueous alteration (Beck et al., 2010). The CM samples with the lowest alteration level would have a broader 3-μm band with a maximum of absorption at higher wavelength, while the CM samples with the highest alteration level would tend to have a narrower 3-μm band with a maximum of absorption at lower wavelength. The spectra of the CIs studied were found to be similar to those of the heavily altered CM chondrites. In order to investigate a possible variation of band shape with aqueous alteration reflectance, the ratio of band depth at 2.8 and 2.9 μm was used, and is compared to the hydrogen content determined by Alexander et al. (2012, 2013) in Fig. 9. In this plot, Allende is a significant outlier and is not shown (outside of the graph range).

A relation between the band shape and the amount of OH/H_2O hydrogen seem to be visible from the reflectance spectra. Following observation in transmission, the band shape is variable across our series of meteorites, with the most hydrated samples having

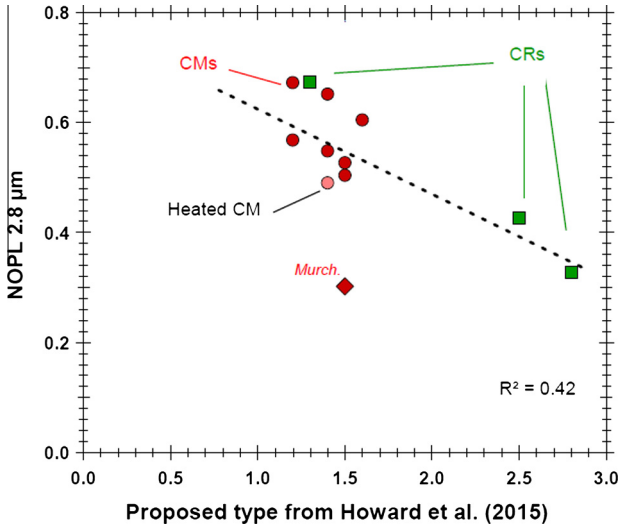

Fig. 8. Correlation between the NOPL at 2.8 μm and the type proposed by Howard et al. (2015).

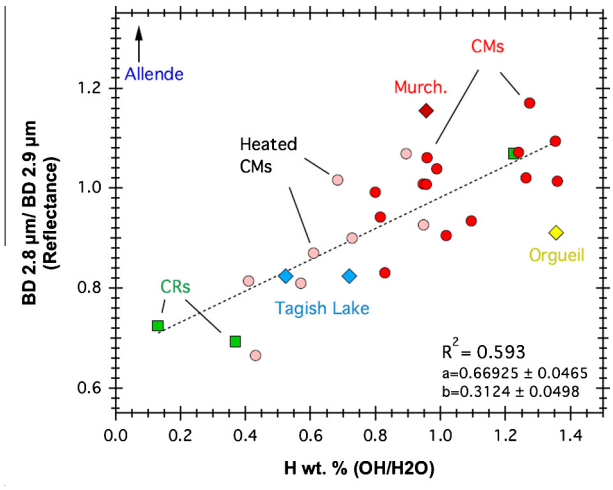

Fig. 9. Evolution of the 3-µm band shape (defined as the ratio between band depths at 2.8 and 2.9 µm) with aqueous alteration extent (probed by H content).

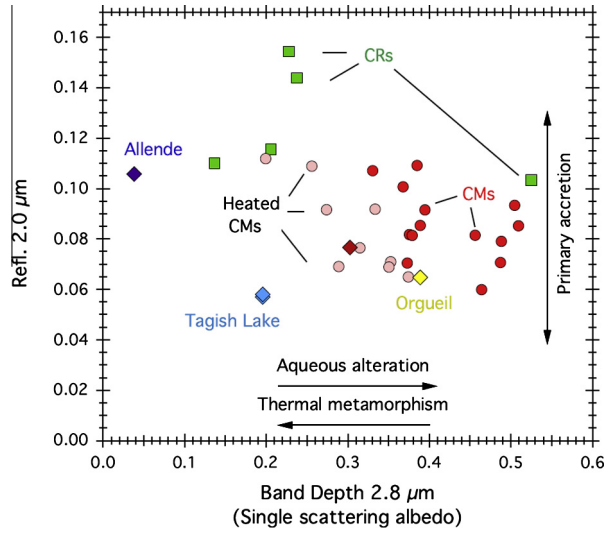

Fig. 10. Reflectance at 2-µm as a function of band depth at 2.8 µm. This diagram enables to separate carbonaceous chondrites groups by their primary properties (e.g. matrix/chondrule ratio) along the *Y* axis and to observe variations related to aqueous alteration within a group along the *X* axis.

a band shape with a band maximum at lower wavelength. Such an evolution of band shape could be related to an evolution of the crystal chemistry of the phyllosilicate with the level of aqueous alteration following a previous proposition (Beck et al., 2010; Howard et al., 2009, 2011). The use of a band shape criterion has some advantage for water quantification since it is virtually independent of reflectance. However the large dispersion of the data in Fig. 9 precludes an accurate quantification.

4.3. Group systematics with reflectance and 3-µm signature

As was discussed previously, the reflectance of carbonaceous chondrites seems to be primarily correlated with the CC group (CI, CM UCC or CR). In addition, several criteria were found to fairly correlate with aqueous alteration level (as probed by OH/H_2O content). In Fig. 10, the reflectance at 2-µm is plotted against the NOPL at 2.8 µm (calculated in single scattering albedo space). Such a graph seems to enable to discriminate at the same time between meteorite groups, as well as between various aqueous alteration levels for a given group. The reflectance appears to be a primary property of a meteorite group (i.e. matrix/chondrule volume ratio) as discussed in part 4.1 and the position along the *X*-axis reflects the extent of aqueous alteration. It would be of certain interest to be able to add to this diagram the various spectroscopic observations of "hydrated" asteroids. However, this would require the knowledge of the spectro-photometric behavior of carbonaceous chondrites. These materials have a non-lambertian behavior (Capaccioni et al., 1990; Beck et al., 2012) and comparing the disk integrated reflectance and band depth to laboratory measurement obtained in standard geometry is incorrect. Using laboratory data obtained under standard conditions will generally lead to an underestimation of continuum reflectance and an overestimation of band depth with respect to disk integrated observations (Pommerol and schmitt, 2008a,b; Beck et al., 2011, 2012). Significant efforts in understanding the spectro-photometric behavior of meteorites might help in improving the connection between primitive meteorites and dark asteroids.

5. Conclusion

In this work, reflectance spectra of 32 carbonaceous chondrites (24 CMs, 5 CRs, 1 CI, 1 CV, Tagish Lake) were measured with high photometric accuracy (<0.0025 in reflectance) in the 0.5–4 µm spectral range. From these data, it is possible to draw the following conclusions regarding the spectral properties of these materials and the capability to infer parent body processes on low albedo asteroids from reflectance spectroscopy.

The reflectance (taken at 2 µm in this work) is roughly correlated with the carbon content for non-heated samples. However, heated CMs while having lost a significant fraction of their carbon do not show a discernable brightening. This suggests that organic carbon related compounds are not the primary darkening agent of carbonaceous chondrites. The extent of aqueous alteration does not seem to affect the reflectance at 2 µm either.

Among the several criteria that were tested to relate the shape of the 3-µm band and the amount of H_2O/OH present in these samples, the normalized optical path length at 2.8 µm is favored (calculated in single scattering albedo space). The correlation is fair and absolute quantification of H_2O/OH from remote sensing of a carbonaceous chondrites parent body using this criterion would have a typical uncertainty of 0.4–0.5 wt% H (i.e. 4–5 wt% H_2O). It is also found that the band shape is changing with the level of aqueous alteration. The spectral criteria we defined (the 2.8–2.9 band depth ratio) evolves with the level of aqueous alteration, as defined by the H_2O/OH content. Such a change is explained by an evolution of the nature and crystal chemistry of the phyllosilicates with aqueous alteration.

Finally, a classification diagram is proposed that enables separation of accretionary properties (i.e. the meteorite group) from parent body processes (aqueous alteration and thermal metamorphism). This can be done using the NOPL at 2.8 µm and the reflectance at 2-µm. Such a diagram could be useful to interpret forthcoming observation of Ceres by the DAWN mission, and could be applied to disk observations of small bodies once the spectro-photometric behavior of carbonaceous chondrites has been measured.

Acknowledgments

The Meteorite Working Group and the Antarctic Meteorite Research Program are acknowledged for providing the samples. Funding and support from CNES, the Programme National de Planétologie as well as Grant ANR-10-JCJC-0505-01 from the

Agence Nationale de la Recherche are acknowledged. KTH was supported by NASA Cosmochemistry Grant NNX14AG27G.

References

Abreu, N.M., Brearley, A.J., 2010. Early Solar System processes recorded in the matrices of two highly pristine CR3 carbonaceous chondrites, MET 00426 and QUE 99177. Geochim. Cosmochim. Acta 74, 1146–1171.

Abreu, N.M., Stanek, G.L., 2009. Chemical consequences of the formation of opaque assemblages on the matrix of CR2 GRA 06100. Meteorit. Planet. Sci. Suppl. 72, 5446 (abstract).

Alexander, C.M.O.D. et al., 2007. The origin and evolution of chondrites recorded in the elemental and isotopic compositions of their macromolecular organic matter. Geochim. Cosmochim. Acta 71, 4380–4403.

Alexander, C.M.O.D. et al., 2012. The provenances of asteroids, and their contributions to the volatile inventories of the terrestrial planets. Science 337, 721–723.

Alexander, C.M.O.D. et al., 2013. The classification of CM and CR chondrites using bulk H, C and N abundances and isotopic compositions. Geochim. Cosmochim. Acta 123, 244–260.

Alexander, C.M.O.d. et al., 2014. Elemental, isotopic, and structural changes in Tagish Lake insoluble organic matter produced by parent body processes. Meteorit. Planet. Sci. 49, 503–525.

Barber, D.J., 1981. Matrix phyllosilicates and associated minerals in C2M carbonaceous chondrites. Geochim. Cosmochim. Acta 45, 945–970.

Beck, P. et al., 2010. Hydrous mineralogy of CM and CI chondrites from infrared spectroscopy and their relationship with low albedo asteroids. Geochim. Cosmochim. Acta 74, 4881–4892.

Beck, P. et al., 2011. Goethite as an alternative origin of the 3.1 μm band on dark asteroids. Astron. Astrophys. 526, A85–A89.

Beck, P. et al., 2012. Photometry of meteorites. Icarus 218, 364–377.

Beck, P. et al., 2014. Transmission infrared spectra (2–25 μm) of carbonaceous chondrites (CI, CM, CV-CK, CR, C2 ungrouped): Mineralogy, water, and asteroidal processes. Icarus 229, 263–277.

Bibring, J.-P. et al., 2006. Global mineralogical and aqueous mars history derived from OMEGA/Mars Express data. Science 312, 400–404.

Bischoff, A. et al., 2006. Nature and origins of meteoritic breccias. In: Lauretta, D.S. (Ed.), Meteorites and the Early Solar System II, pp. 679–712.

Brearley, A.J., 2006. The action of water. In: Bonzel, R.P. et al. (Eds.), Meteorites and the Early Solar System II. The University of Arizona Science Series, Tucson, pp. 587–623.

Brissaud, O. et al., 2004. Spectrogonio radiometer for the study of the bidirectional reflectance and polarization functions of planetary surfaces. 1. Design and tests. Appl. Opt. 43, 1926–1937.

Browning, L.B., McSween, H.Y., Zolensky, M.E., 1996. Correlated alteration effects in CM carbonaceous chondrites. Geochim. Cosmochim. Acta 60, 2621–2633.

Bunch, T.E., Chang, S., 1980. Carbonaceous chondrites-II. Carbonaceous chondrite phyllosilicates and light element geochemistry as indicators of parent body processes and surface conditions. Geochim. Cosmochim. Acta 44, 1543–1577.

Burbine, T.H., 1998. Could G-class asteroids be the parent bodies of the CM chondrites? Meteorit. Planet. Sci. 33, 253–258.

Bus, S.J., Binzel, R.P., 2002. Phase II of the small main-belt asteroid spectroscopic survey a feature-based taxonomy. Icarus 158, 146–177.

Campins, H. et al., 2010. Water ice and organics on the surface of the Asteroid 24 Themis. Nature 464, 1320–1321.

Capaccioni, F. et al., 1990. Phase curves of meteorites and terrestrial rocks – Laboratory measurements and applications to asteroids. Icarus 83, 325–348.

Carter, J. et al., 2010. Detection of hydrated silicates in crustal outcrops in the Northern Plains of Mars. Science 328, 1682–1686.

Clark, R.N., Roush, T.L., 1984. Reflectance spectroscopy – Quantitative analysis techniques for remote sensing applications. J. Geophys. Res. 89, 6329–6340.

Cloutis, E.A. et al., 2011a. Spectral reflectance properties of carbonaceous chondrites: 3. CR chondrites. Icarus 217, 389–407.

Cloutis, E.A. et al., 2011b. Spectral reflectance properties of carbonaceous chondrites: 2. CM chondrites. Icarus 216, 309–346.

Cloutis, E.A. et al., 2012. Spectral reflectance properties of carbonaceous chondrites: 6. CV chondrites. Icarus 221, 328–358.

Cord, A.M. et al., 2003. Planetary regolith surface analogs: Optimized determination of Hapke parameters using multi-angular spectro-imaging laboratory data. Icarus 165, 414–427.

Cord, A.M. et al., 2005. Experimental determination of the surface photometric contribution in the spectral reflectance deconvolution processes for a simulated martian crater-like regolithic target. Icarus 175, 78–91.

DeMeo, F.E., Carry, B., 2014. Solar System evolution from compositional mapping of the asteroid belt. Nature 505, 629–634.

DeMeo, F.E. et al., 2009. An extension of the Bus asteroid taxonomy into the near-infrared. Icarus 202, 160–180.

Gaffey, M.J., Burbine, T.H., Binzel, R.P., 1993. Asteroid spectroscopy – Progress and perspectives. Meteoritics 28, 161–187.

Garenne, A. et al., 2014. The abundance and stability of "water" in type 1 and 2 carbonaceous chondrites (CI, CM and CR). Geochim. Cosmochim. Acta 137, 93–112.

Gilmour, I., 2003. Structural and isotopic analysis of organic matter in carbonaceous chondrites. In: Davis, A.M. (Ed.), Meteorites, Comets and Planets, vol. 1. Elsevier-Pergamon, pp. 269–290.

Hapke, B., 2012. Theory of Reflectance and Emittance Spectroscopy, second ed. Cambridge University Press, New York.

Harju, E.R., Rubin, A.E., 2013. GRO 95577 and MIL 090292: The most aqueously altered CR chondrites. Meteorit. Planet. Sci. Suppl. 76, 5250 (abstract).

Howard, K.T. et al., 2009. Modal mineralogy of CM2 chondrites by X-ray diffraction (PSD-XRD). Part 1: Total phyllosilicate abundance and the degree of aqueous alteration. Geochim. Cosmochim. Acta 73, 4576–4589.

Howard, K.T. et al., 2010. Modal mineralogy of CV3 chondrites by X-ray diffraction (PSD-XRD). Geochim. Cosmochim. Acta 74, 5084–5097.

Howard, K.T. et al., 2011. Modal mineralogy of CM chondrites by X-ray diffraction (PSD-XRD): Part 2. Degree, nature and settings of aqueous alteration. Geochim. Cosmochim. Acta 75, 2735–2751.

Howard, K.T. et al., 2015. Classification of hydrous meteorites (CR, CM and C2 ungrouped) by phyllosilicate fraction: PSD-XRD modal mineralogy and planetesimal environments. Geochim. Cosmochim. Acta 149, 206–222.

Jones, T.D. et al., 1990. The composition and origin of the C, P, and D asteroids – Water as a tracer of thermal evolution in the outer belt. Icarus 88, 172–192.

Jouglet, D. et al., 2007. Hydration state of the martian surface as seen by Mars Express OMEGA: 1. Analysis of the 3 μm hydration feature. J. Geophys. Res. (Planets) 112, p. E08S06.

Kortum, G., 1969. Reflectance Spectroscopy. Springer, New York, pp. 366.

Krot, A.N. et al., 2007. Classification of meteorites. In: Treatise on Geochemistry. Elsevier.

Lair, V. et al., 2006. Electrochemical reduction of ferric corrosion products and evaluation of galvanic coupling with iron. Corros. Sci. 48, 2050–2063.

Larson, H.P., Feierberg, M.A., Lebofsky, L.A., 1983. The composition of Asteroid 2 Pallas and its relation to primitive meteorites. Icarus 56, 398–408.

Lebofsky, L.A. et al., 1981. The 1.7- to 4.2-micron spectrum of Asteroid 1 Ceres – Evidence for structural water in clay minerals. Icarus 48, 453–459.

McSween, H.Y., 1979. Alteration in CM carbonaceous chondrites inferred from modal and chemical variations in matrix. Geochim. Cosmochim. Acta 43, 1761–1765.

McSween Jr., H.Y., Ghosh, A., Weidenschilling, S.J., 2002. Accounting for the thermal structure of the asteroid belt: Where are we now? Meteorit. Planet. Sci. Suppl. 37, 98 (abstract).

Milliken, R.E., Mustard, J.F., 2005. Quantifying absolute water content of minerals using near-infrared reflectance spectroscopy. J. Geophys. Res. (Planets) 110, p. E12001.

Milliken, R.E., Mustard, J.F., 2007. Estimating the water content of hydrated minerals using reflectance spectroscopy. I. Effects of darkening agents and low-albedo materials. Icarus 189, 550–573.

Moroz, L.V. et al., 1998. Natural solid bitumens as possible analogs for cometary and asteroid organics: 1. Reflectance spectroscopy of pure Bitumens. Icarus 134, 253–268.

Mustard, J.F., Hays, J.E., 1997. Effects of hyperfine particles on reflectance spectra from 0.3 to 25 μm. Icarus 125, 145–163.

Orthous-Daunay, F.R. et al., 2013. Mid-infrared study of the molecular structure variability of insoluble organic matter from primitive chondrites. Icarus 223, 534–543.

Pommerol, A., Schmitt, B., 2008a. Strength of the H_2O near-infrared absorption bands in hydrated minerals: Effects of particle size and correlation with albedo. J. Geophys. Res. (Planets) 113, p. E10009.

Pommerol, A., Schmitt, B., 2008b. Strength of the H_2O near-infrared absorption bands in hydrated minerals: Effects of measurement geometry. J. Geophys. Res. (Planets) 113, p. E12008.

Quirico, E., Orthous-daunay, F.-R., Beck, P., Bonal, L., Brunetto, R., Dartois, E., Pino, T., Montagnac, G., Rouzaud, J.-N., Engrand, C., Duprat, J., 2014. Origin of insoluble organic matter in type 1 and 2 chondrites: New clues, new questions. Geochim. Cosmochim. Acta. 136, 80–99.

Remusat, L. et al., 2006. Enrichment of deuterium in insoluble organic matter from primitive meteorites: A Solar System origin? Earth Planet. Sci. Lett. 243, 15–25.

Rivkin, A.S., Emery, J.P., 2010. Detection of ice and organics on an asteroidal surface. Nature 464, 1322–1323.

Rivkin, A.S., Davies, J.K., Johnson, J.R., Ellison, S.L., Trilling, D.E., Brown, R.H., Lebofsky, L.A., 2003. Hydrogen concentrations on C-class asteroids derived from remote sensing. Meteorit. Planet. Sci. 38, 1383–1398.

Rivkin, A. et al., 2002. Hydrated minerals on asteroids: The astronomical record. In: Asteroids III. University of Arizona Press, Tucson, pp. 235–253.

Rubin, A.E. et al., 2007. Progressive aqueous alteration of CM carbonaceous chondrites. Geochim. Cosmochim. Acta 71, 2361–2382.

Scott, E.R.D., Krot, A.N., 2007. Chondrites and their components. Treatise on Geochemistry. Elsevier.

Shkuratov, Y.G., Grynko, Y.S., 2005. Light scattering by media composed of semitransparent particles of different shapes in ray optics approximation: Consequences for spectroscopy, photometry, and polarimetry of planetary regoliths. Icarus 173, 16–28.

Takir, D., Emery, J.P., 2012. Outer main belt asteroids: Identification and distribution of four 3-μm spectral groups. Icarus 219, 641–654.

Takir, D. et al., 2013. Nature and degree of aqueous alteration in CM and CI carbonaceous chondrites. Meteorit. Planet. Sci. 48, 1618–1637.

Tholen, D.J., 1984. Asteroid Taxonomy from Cluster Analysis of Photometry. Ph.D. Thesis, Arizona Univ., Tucson.

Tomeoka, K., Buseck, P.R., 1985. Indicators of aqueous alteration in CM carbonaceous chondrites: Microtextures of a layered mineral containing Fe, S, O and Ni. Geochim. Cosmochim. Acta 49, 2149–2163.

Tomeoka, K., Buseck, P.R., 1988. Matrix mineralogy of the Orgueil CI carbonaceous chondrite. Geochim. Cosmochim. Acta 52, 1627–1640.
Tomeoka, K., McSween Jr., H.Y., Buseck, P.R., 1989. Mineralogical alteration of CM carbonaceous chondrites: A review. Antarct. Meteor. Res. 2, 221–234.
Vilas, F., 1994. A cheaper, faster, better way to detect water of hydration on Solar-System bodies. Icarus 111, 456–467.
Weisberg, M.K., Huber, H., 2007. The GRO 95577 CR1 chondrite and hydration of the CR parent body. Meteorit. Planet. Sci. 42, 1495–1503.
Zolensky, M., McSween Jr., H.Y., 1988. Aqueous alteration. In: Kerridge, J.F., Matthews, M.S. (Eds.), Meteorites and the Early Solar System. The University of Arizona Press, Tucson, AZ, pp. 114–143.